tvst

https://doi.org/10.1167/tvst.7.1.19

Article

Detecting Glaucomatous Progression With a Region-of-Interest Approach on Optical Coherence Tomography: A Signal-to-Noise Evaluation

Zhichao Wu[1–3], Abinaya Thenappan[1], Denis S. D. Weng[1], Robert Ritch[4], and Donald C. Hood[1,5]

[1] Department of Psychology, Columbia University, New York, NY, USA
[2] Center for Eye Research Australia, Royal Victorian Eye and Ear Hospital, East Melbourne, Australia
[3] Ophthalmology, Department of Surgery, The University of Melbourne, Melbourne, Australia
[4] Einhorn Clinical Research Center, New York Eye and Ear Infirmary of Mount Sinai, New York, NY, USA
[5] Department of Ophthalmology, Columbia University, New York, NY, USA

Correspondence: Zhichao Wu, Center for Eye Research Australia, Level 7, 32 Gisborne St, E Melbourne, VIC 3002, Australia. e-mail: wu.z@unimelb.edu.au

Received: 16 November 2017
Accepted: 24 December 2017
Published: 28 February 2018

Keywords: glaucoma; optical coherence tomography; progression; region-of-interest

Citation: Wu Z, Thenappan A, Weng DSD, Ritch R, Hood DC. Detecting glaucomatous progression with a region-of-interest approach on optical coherence tomography: a signal-to-noise evaluation. Trans Vis Sci Tech. 2018;7(1):19, https://doi.org/10.1167/tvst.7.1.19

Purpose: To compare two region-of-interest (ROI) approaches and a global thickness approach for capturing progressive circumpapillary retinal nerve fiber layer (cpRNFL) changes on optical coherence tomography (OCT) imaging.

Methods: Progressive cpRNFL thickness changes were evaluated in 164 eyes with a clinical diagnosis of glaucoma or suspected glaucoma; all eyes underwent optic disc OCT imaging on two visits at least 1 year apart. Such changes were evaluated with a manual ROI approach (ROI_M), which involved manual identification of region(s) of observed or suspected glaucomatous damage. The ROI_M was compared with an automatic ROI approach (ROI_A), where regions were automatically identified if the cpRNFL thickness fell below the 1% lower normative limits, and to global cpRNFL thickness. These methods were compared using longitudinal signal-to-noise ratios (SNRs), calculated based upon individualized estimates of measurement variability and age-related changes for each ROI, obtained from 321 glaucoma eyes and 394 healthy eyes, respectively.

Results: The average longitudinal SNR of the ROI_M, ROI_A and global thickness methods were -0.46, -0.39, and -0.30 y^{-1}, respectively. The average longitudinal SNR for the ROI_M was significantly more negative compared with both the ROI_A and global thickness methods ($P = 0.005$ for both).

Conclusions: A manual ROI approach was the optimal method for detecting progressive cpRNFL loss compared with an automatic ROI approach and the global cpRNFL thickness measure.

Translational Relevance: These findings highlight the potential advantages conferred by a careful qualitative evaluation of OCT imaging for detecting glaucoma progression.

Introduction

Accurate detection of disease progression is crucial to the clinical management of glaucoma, as it is important for risk assessment and to tailor therapy needed to prevent the development or worsening of functional disability.[1] Progressive worsening is a hallmark feature of glaucoma, and identifying eyes where it occurs significantly can contribute to the certainty of its diagnosis, in cases where that is in question.[2,3] However, detecting progression continues to be a challenge in the clinical management of patients with glaucoma.

Optical coherence tomography (OCT) imaging has been increasingly used in clinical practice for the detection of glaucomatous progression. Common OCT methods used to evaluate progression include

global trend-based analysis of the average retinal nerve fiber layer (RNFL) thickness of a circumpapillary circle scan and topographic event–based analysis of an RNFL thickness map.[4] Recent studies have also demonstrated the potential of topographic trend–based analysis.[5,6] Currently, all these methods consider progression to have occurred after a specific set of criteria have been met (e.g., statistically significant change in a number of contiguous superpixels), which could occur simply as a result of measurement variability.

We hypothesize that it may be possible to improve the accuracy of detecting progression by evaluating regions with glaucomatous damage, because such regions are by nature a result of progression. Our previous studies[7,8] provide preliminary evidence for this, showing that evaluating progression in such region(s)-of-interest (ROI) performed better than using an average circumpapillary RNFL (cpRNFL) thickness measurement. However, these ROIs were automatically identified in our previous studies, which may miss glaucomatous damage that might be visible (and thus manually identified) through a qualitative evaluation of the OCT imaging results.[9]

Therefore, in this study, we compared the ability of three approaches for distinguishing OCT changes over time from normal age-related changes[10–12] and measurement variability.[13–15] In particular, we evaluated regions of observed or suspected glaucomatous damage determined manually, and compared the results with typically used global parameters and with automatically defined regions of abnormalities.

Methods

Study Overview

As an overview (with details described further below), this study compared three approaches for detecting progressive cpRNFL thickness changes: (1) a global thickness approach, (2) an automatic ROI approach, and (3) a manual ROI approach. Eyes with suspected or established glaucoma based on a comprehensive clinical examination by the referring glaucoma specialist (RR) were evaluated. To examine cpRNFL thickness changes over time, the comparison of these approaches was performed in eyes with at least two OCT scans $\geq$1 year apart ("longitudinal group"). The cpRNFL thickness changes detected by each approach were then normalized so that equivalent comparisons could be performed. This normalization process required individualized estimates of measurement variability, derived from a cohort of eyes with glaucoma or suspected glaucoma that had two OCT scans during the same visit (a "variability group"). The normalization process also required individualized estimates of normal age-related changes, derived from a cohort of eyes from healthy participants with one OCT scan at cross-section (a "normative group"). The normalized values are referred to as longitudinal signal-to-noise ratios (SNRs), which was the primary outcome measure used in this study.

Participants with Suspected or Established Glaucoma

Participants with suspected or established glaucoma evaluated as part of a prospective study to evaluate the role of OCT imaging in glaucoma were included, and this study was approved by the institutional review boards of Columbia University and the New York Eye and Ear Infirmary of Mount Sinai and adhered with the Declaration of Helsinki and the Health Insurance Portability and Accountability Act. Written informed consent was obtained from all participants after an explanation of the study. All eyes were required to have at least one reliable visual field test performed using the Swedish Interactive Threshold Algorithm (SITA) standard 24-2 testing strategy on a Humphrey Field Analyzer II-I (Carl Zeiss Meditec, Inc., Dublin, CA). A visual field test was considered unreliable if greater than 33% fixation losses or false-negative errors (except for the latter when mean deviation [MD] was <-12 dB), or greater than 15% false-positive errors were present. Any eye with retinal pathology that could affect the cpRNFL (e.g., epiretinal membranes, retinoschisis) was excluded. Volume scans consisting of 512×128 A-scans over a 6×6-mm region centered on the optic disc were obtained for the glaucoma eyes using a spectral-domain (SD) OCT device (3D OCT-2000; Topcon, Inc., Tokyo, Japan). Any scan affected by significant blink or eye movement artifacts was excluded. All glaucoma eyes were required to have at least two scans either: (1) greater than or equal to 1 year apart to determine change over time (or "signal"), or (2) during the same visit to determine test–retest variability (or "noise"). Eyes meeting these criteria formed the "longitudinal group" and "variability group," respectively. If an eye fulfilled both criteria, they were assigned to the "longitudinal group" in this study.

Healthy Participants

One randomly selected eye each from 394 healthy participants was also included in this study to provide cross-sectional estimates of normal age-related changes in the cpRNFL thickness, and formed the "normative group" in this study. These healthy eyes were part of a study to determine normal reference limits by the OCT device manufacturer (data provided by Topcon, Inc.). Briefly, all eyes were required to be free of any ocular pathology, have a best-corrected visual acuity of 20/40 or better, and have an intraocular pressure of less than or equal to 21 mm Hg. Eyes were excluded if visual field defects consistent with glaucoma were present on a test when using the SITA Standard 24-2 strategy, narrow angles, and patients were excluded if they had a significant medical history that could influence test results. The same OCT volume scan protocol was used for these healthy eyes as were used for the glaucoma eyes, with the exception that a different SD-OCT device was used (3D OCT-1 Maestro; Topcon, Inc.). The only key difference between the two devices is the scan acquisition speed (27,000 and 50,000 A-scans per second for the 3D OCT-2000 and 3D OCT-1 Maestro, respectively). The median (interquartile range [IQR]) age of these healthy participants was 47 years (IQR = 32–60 years), and the median global cpRNFL thickness of these eyes was 104 μm (96–111 μm).

Methods to Detect Progression Over Time using the Circumpapillary Circle Scan

Using a customized program on MATLAB (MathWorks Inc., Natick, MA), the two scans of each eye in these two groups (longitudinal and variability groups) were manually aligned with each other using retinal features (including the optic disc and blood vessels) visible on the en face projection images. Following image alignment, a circle scan centered on the optic disc was derived at the same location for both scans, having a diameter of 3.4 mm and averaged over an annulus of 100 μm in width.[7,8]

Three methods were used to evaluate progressive changes in the cpRNFL thickness over time for eyes in the longitudinal group. The first involved comparing the change in global thickness over time, and the second compared the average thickness of region(s) of the cpRNFL that fell below its 1% normal limits over at least 5° of the cpRNFL as identified on the second visit, with the average thickness of the same region(s) on the first visit.[7,8] The latter method can be described as an automatic ROI approach (ROI_A). The third method is similar to the ROI_A approach, but instead involves a manual outlining of region(s) of observed or suspected glaucomatous damage on the circle scan or cpRNFL thickness profile, after reviewing information available from the volume scan of the optic disc. We refer this as the manual ROI approach (ROI_M). An experienced grader performed this manual identification, using only the information from the second visit. They were masked to the information from the first visit in order to avoid bias of simply choosing regions that exhibited a decline. This evaluation was performed using a customized program on MATLAB, where six components from the volume scan of the optic disc, shown in Figure 1, were used: (i) a fundus projection image; (ii) an en face slab image of the inner retina, which was the average intensity in a 52-μm slab below the inner limiting membrane[16]; (iii) an RNFL thickness plot; (iv) an RNFL thickness deviation probability plot; (v) an OCT image of the derived circle B-scan; and (vi) its corresponding RNFL thickness profile. For both the ROI approaches, it is possible that some eyes did not have any regions that met the criterion with the ROI_A approach, or the grader did not consider that an eye had a region of glaucomatous damage with the ROI_M approach. In either case, the entire cpRNFL thickness profile was considered the ROI to be evaluated for change over time because it would still be important to determine whether cpRNFL thickness changes were occurring at a global level even if no ROIs were identified, and thus the global thickness measurement was used.

Deriving the Longitudinal Signal-to-Noise Ratios

To compare these approaches, we need to account for the between-method and between-individual differences in measurement variability and normal age-related changes. To this end, we calculated longitudinal signal-to-noise ratios (SNRs).[17] The longitudinal SNR of the change in cpRNFL thickness over time was derived for each method (m) by dividing its change (δ) by the duration between tests (t), before subtracting a corresponding estimate of age-related change (a). This value was then divided by an estimate of variability (σ). This process can be summarized as follows:

$$SNR_m = \frac{(\delta_m/t) - a_m}{\sigma_m} \quad (1)$$

Because the ROI approaches evaluate change in regions that are unique to each eye, individualized estimates of age-related change and variability were required.

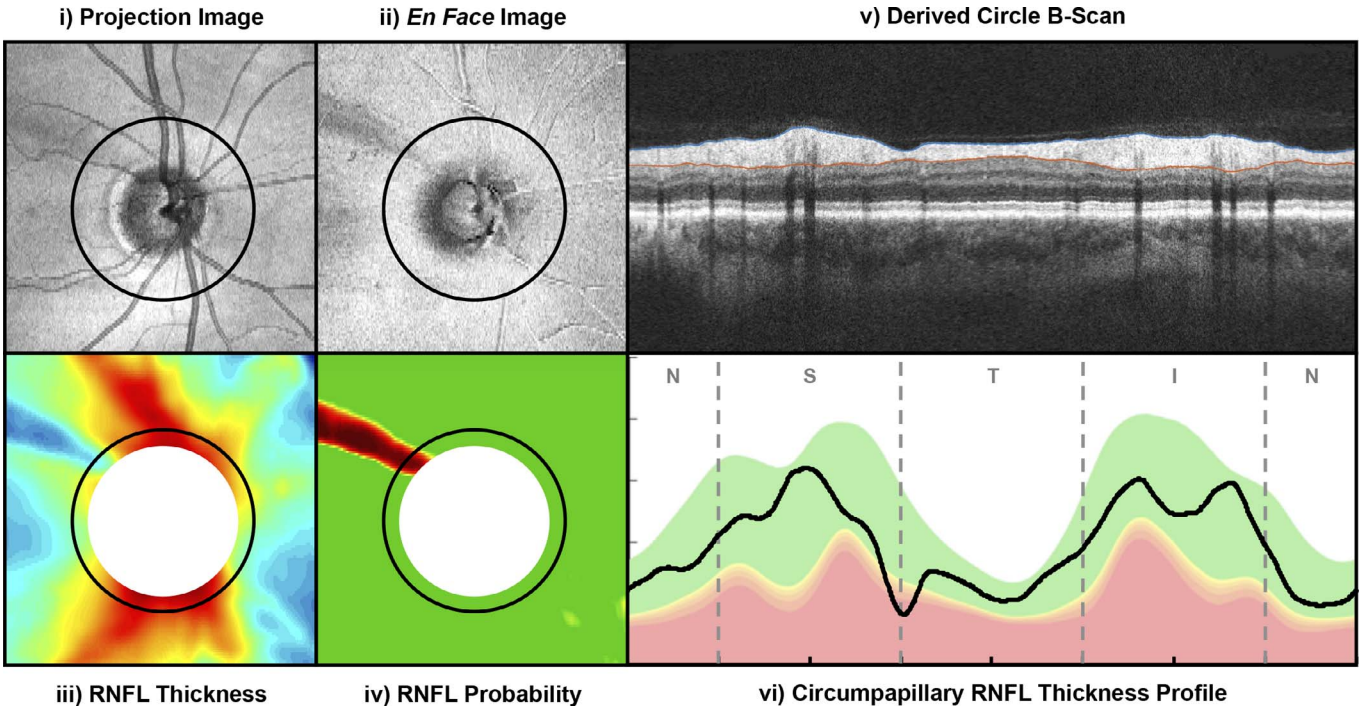

Figure 1. Information from the volume scan centered on the optic disc used to manually determine an ROI: (i) fundus projection image; (ii) en face slab image of the inner retina; (iii) RNFL thickness plot; (iv) RNFL thickness deviation probability plot; (v) derived circle B-scan; and (vi) the corresponding cpRNFL thickness profile (*bottom right*).

The process used to obtain individualized age-related change (a) and variability estimates (σ) for each of the ROI(s) of a given eye in the longitudinal group is illustrated in Figure 2. In this example, a superior-temporal cpRNFL defect was the ROI for this eye in the longitudinal group, as shown by a green arc (left section). An individualized age-related change estimate for this ROI was then obtained by first deriving the average RNFL of the same region in each eye of the normative group (shown by the green arcs in the middle section), then calculating the slope of a linear regression fitted to these values against age. Individualized variability estimates were obtained also by first deriving the test–retest difference of the average RNFL of the same region in each eye of the variability group (also shown by the green arcs in the right section), and then calculating the standard deviation (SD) of these differences from the entire group (see Statistical Analysis section). This process was repeated for all ROIs in all eyes of the longitudinal group.

Statistical Analysis

The SD of the test–retest difference for each ROI was calculated using a random intercept model (a type of linear mixed model) in order to account for the hierarchical nature of the test–retest differences (i.e., that two eyes from the same participant could be included). Comparisons of the difference in the average longitudinal SNR between methods were also performed using random intercept models when nesting the methods within eyes and within participants. Statistical analyses were performed using both MATLAB and Stata (StataCorp LP, College Station, TX).

Results

Participant Characteristics

A total of 164 eyes from 96 participants diagnosed with glaucoma or suspected glaucoma were included in the longitudinal group, and their median (IQR) age and follow-up duration were 61 years (IQR = 50–68 years) and 1.6 years (IQR = 1.1–2.0 years), respectively. The median visual field MD and pattern standard deviation (PSD) of these eyes were −2.53 dB (−4.94 to −0.57 dB) and 2.07 dB (1.59–5.71 dB), respectively. The median baseline and rate of change for global RNFL thickness of these eyes was 85 µm (66–97 µm) and −0.8 µm/y (−2.3 to 0.5 µm/y), respectively. The median rate of cpRNFL thickness

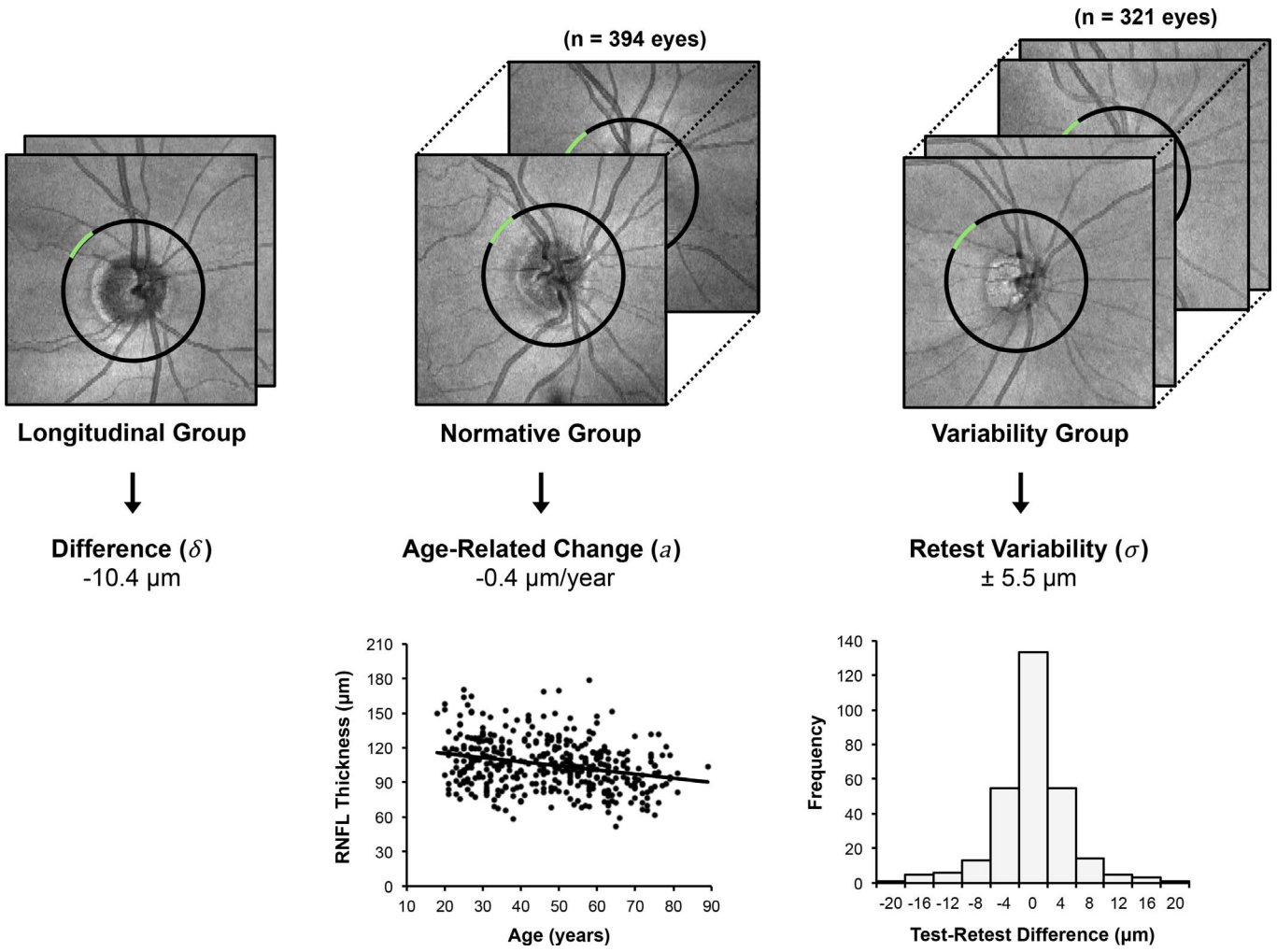

Figure 2. Illustration of the process to derive estimates of age-related change and measurement variability of the cpRNFL thickness for a specific ROI (*green region*) of the derived circle scan (*black circle*) for each eye in the longitudinal group. Age-related change estimates are obtained by estimating the slope of the linear regression fit between cpRNFL thickness values of a particular ROI and age of all eyes in the "normative group." Measurement variability estimates are obtained by calculating the standard deviation of the test-retest difference of the cpRNFL thickness of the same ROI for eyes in the "variability group."

change using the ROI_A and ROI_M approaches was −1.5 µm/y (−3.3 to 0.1 µm/y) and −1.7 µm/y (−3.7 to −0.1 µm/y), respectively. This study also included of 321 eyes from 199 participants diagnosed with glaucoma or suspected glaucoma in the variability group with a median age of 62 years (IQR = 49–69 years), and the median visual field MD and PSD of these eyes were −2.57 dB (−6.04 to −0.90 dB) and 2.27 (1.55–6.54 dB), respectively.

Properties of the Regions-of-Interest Outlined

The spatial location and extent of the automatically and manually outlined ROIs for all the eyes in the longitudinal cohort are plotted in Supplementary Figure (with red and blue lines, respectively). Among the eyes where an ROI was outlined by either method (n = 109), the median total width of the ROI(s) outlined using the automatic and manual approaches were 50° (IQR = 20°–90°) and 62° (IQR = 34°–101°). The median proportion of overlap between the ROI(s) selected by the two methods were 57% (IQR = 41%–81%), with only 29 eyes (or 27%) showing an overlap of greater than 80%. This can be attributed to scenarios when multiple automatically identified ROIs were manually outlined as one single ROI, or when an examiner manually outlined an ROI on the basis that a region of observed or suspected glaucomatous damage was present that was not automatically identified, and vice versa.

Comparison of the Longitudinal Signal-to-Noise Ratio Between Methods

The distribution of the longitudinal SNRs of each eye for each method is shown using in Figure 3. The average longitudinal SNRs for the ROI_M, ROI_A and global thickness methods were −0.46, −0.39, and −0.30 y^{-1}, respectively. Recall that a more negative value indicates a greater degree of cpRNFL loss relative to normal age-related and measurement variability. These findings demonstrate that the ROI_M approach performed better compared with the ROI_A or global thickness methods. More specifically, the average longitudinal SNR for the ROI_M was significantly more negative compared with the ROI_A (−0.07 y^{-1}; 95% confidence interval [CI] = −0.12 to −0.02 y^{-1}, $P = 0.005$) and global thickness (−0.15 y^{-1}; 95% CI = −0.26 to −0.05 y^{-1}, $P = 0.005$). Note that even though the average longitudinal SNR of the ROI_A approach was more negative than the global thickness parameter, the difference did not reach statistical significance (−0.08 y^{-1}; 95% CI = −0.20 to 0.03 y^{-1}, $P = 0.167$).

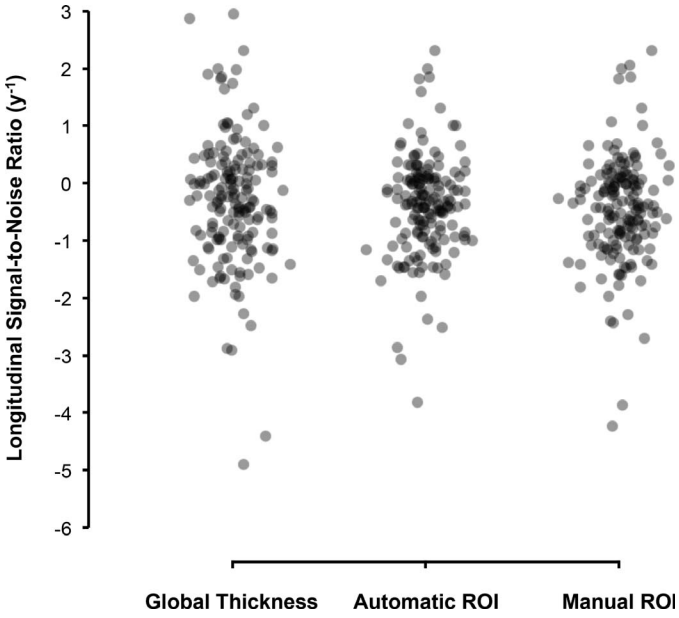

Figure 3. Distribution of the longitudinal SNR) of the global thickness, automatic and manual ROI approaches, with more negative values indicating a greater degree of cpRNFL thinning over time relative to age-related changes and measurement variability.

Examples of Findings in this Study

Below are four examples to illustrate the possible basis for the superior ability of the ROI_M approach for detecting progression. The first two examples illustrate how both the ROI_M and ROI_A performed better than the global thickness approach when progressive cpRNFL thickness changes occurred at a localized region. The first case (Fig. 4A) shows an eye with an inferior-temporal RNFL defect, where the manually outlined region (shown as black rectangles in the middle and bottom rows) corresponded closely with the automatically defined ROI (note that most of the cpRNFL thickness decline occurred in this local region). Thus, it is not surprising that the longitudinal SNR of the ROI_M (−2.4 y^{-1}) and ROI_A (−2.5 y^{-1}) methods were more negative than that of the global thickness method (−0.6 y^{-1}). The second case (Fig. 4B) shows an eye with both a superior-temporal and inferior-temporal RNFL defect, where the manually marked (shown as black rectangles in the middle and bottom rows) and automatically defined regions again corresponded closely. In this case, cpRNFL thickness changes primarily occurred in the inferior-temporal region, and the longitudinal SNR of the ROI_M, ROI_A and global thickness methods were −1.7, −1.7, and −1.2 y^{-1}, respectively.

The next two examples illustrate how the ROI_M method can perform better than both the ROI_A and global thickness approaches when a region appears abnormal, but does not fall below the 1% lower normative limits (red region). The third case (Fig. 5A) presents an eye in which glaucomatous damage was suspected in the superior-temporal region (manually outlined with black rectangles in the middle and bottom rows), on the basis of the RNFL thickness and probability plots and its appearance on the derived circle B-scan, although this region did not meet the criterion used to identify an automatic ROI (i.e., it did not fall below the 1% lower normative limits). A decrease in the cpRNFL thickness in this region occurred over time, and thus the longitudinal SNR of the ROI_M (−1.2 y^{-1}) was more negative than the ROI_A method, which did not identify an abnormal region or the global thickness method (−0.3 y^{-1}). The fourth case (Fig. 5B) presents an eye where glaucomatous damage was observed in the inferior-temporal region (manually outlined with black rectangles in the middle and bottom rows), visible on the en face slab image, RNFL thickness plot, derived circle B-scan and the cpRNFL thickness profile as a localized defect (white arcs in upper panels of Fig. 5B). However, this defect did not fall below the 1% lower normative limits, and was thus missed when using the automatic ROI approach. Therefore,

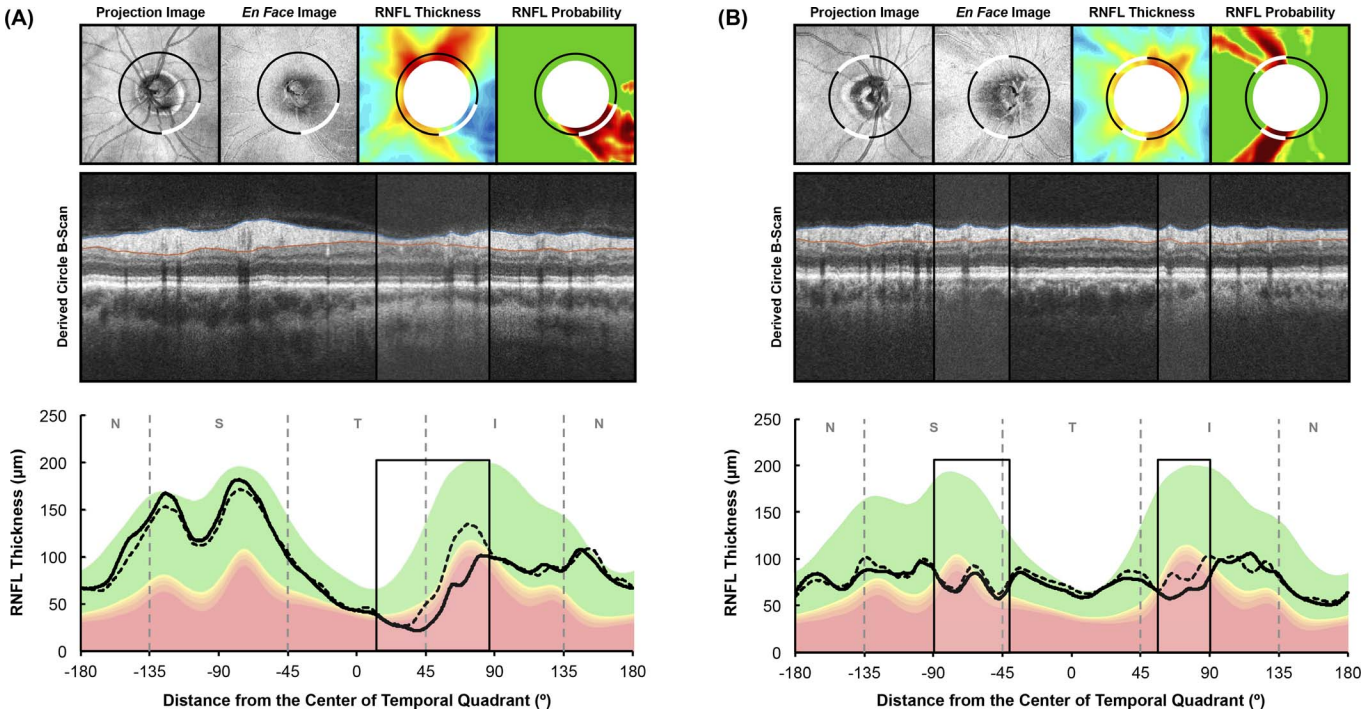

Figure 4. Two examples illustrating how an ROI approach performed better than the global thickness parameter for capturing changes in the cpRNFL thickness. In each example, the *top row* shows the fundus projection image, en face slab image, RNFL thickness plot, and RNFL thickness deviation probability plots respectively (*left* to *right*). The *middle* and *bottom rows* present the derived circle B-scan and the cpRNFL thickness profile, respectively. The location from where the circle scan was derived are shown as the *black circles* on the *top row*, and the manually outlined ROI are represented by the *white region*, corresponding to the region outlined by the *black rectangles* in the *middle* and *bottom rows*.

the longitudinal SNR of this eye using the ROI_M method was more negative ($-2.4\ y^{-1}$) than with the global thickness method ($-1.6\ y^{-1}$).

Discussion

This study demonstrated that a manual ROI approach improved the ability to distinguish glaucoma-associated changes in the cpRNFL thickness from normal age-related changes and measurement variability compared with the conventional metric of global thickness. Furthermore, this approach, which makes use of a prior knowledge of patterns of glaucomatous damage during the qualitative assessment, also performed better than an automatic ROI approach that relies on a predefined criterion. These findings highlight how making full use of the available OCT imaging information can optimize the detection of progressive cpRNFL thickness changes.

The methods of this study differ from those of our two previous studies[7,8] that demonstrated that the width of an ROI, which was defined using the 1% lower normative limits of cpRNFL thickness, increased significantly over time at the population level, in eyes where the global cpRNFL did not exhibit a statistically significant decline. First, we studied a substantially larger group of glaucoma eyes, and did not restrict our sample to eyes with disc hemorrhages as we did in our first study.[7] Second, we included a method where regions of observed or suspected glaucomatous damage were manually outlined and evaluated for progressive changes, because such regions may not always be captured using the automatic ROI approach. Third, we evaluated the average cpRNFL in an ROI instead of simply measuring the width of an ROI, because glaucomatous damage often results in both a deepening and widening of a cpRNFL defect. Finally, we ensured that the ROI and global cpRNFL thickness measures were equivalently compared by computing longitudinal SNRs[17] after adjustments for measurement variability and age-related changes. The latter is important as the measurement variability is higher[13–15] and age-related changes differ for localized

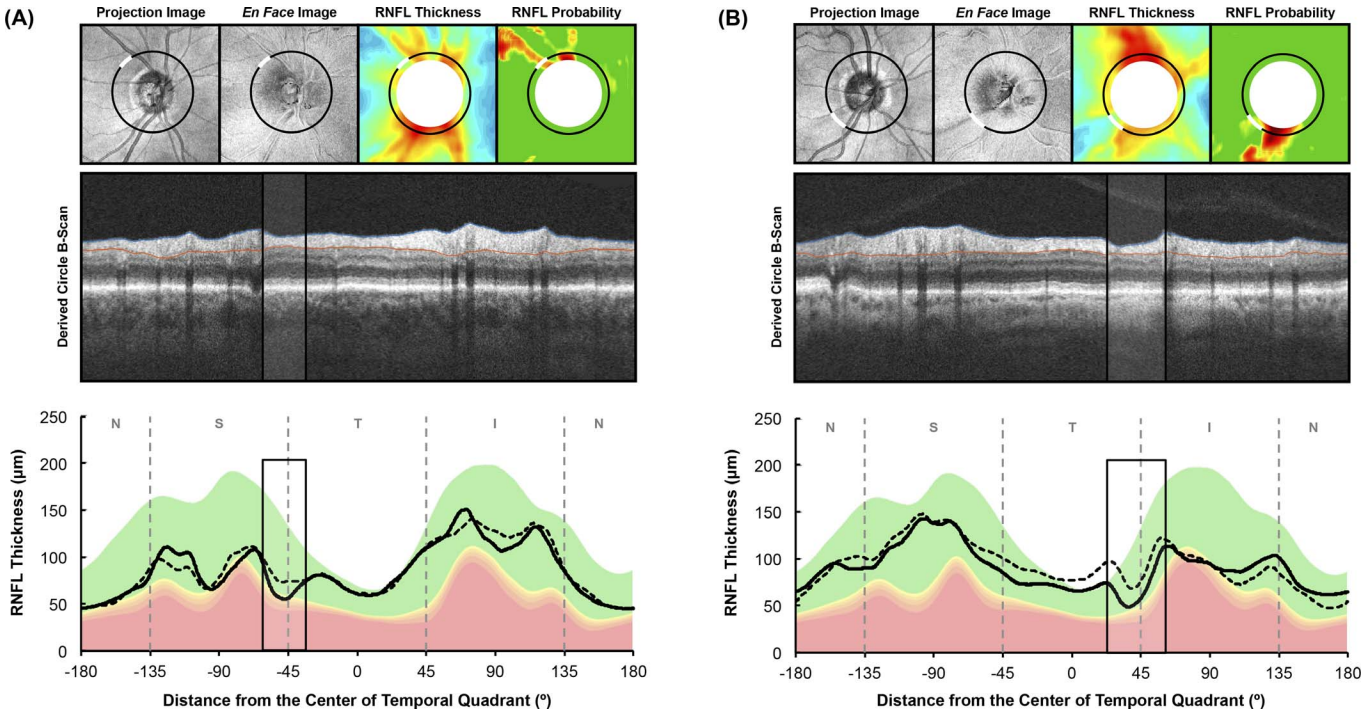

Figure 5. Two examples illustrating how a manual ROI approach performed better than both the automatic ROI approach and the global thickness parameter for capturing changes in the cpRNFL thickness that did not fall below the 1% lower normative limits (*red region*). In each example, the *top row* presents the fundus projection image, en face slab image, RNFL thickness plot and RNFL thickness deviation probability plots, respectively (*left* to *right*). The *middle* and *bottom rows* show the derived circle B-scan and the cpRNFL thickness profile, respectively. The location from where the circle scan was derived are indicated by *black circles* on the *top row*, and the manually outlined ROI are represented by the *white arcs*, which corresponds to region outlined by the *black boxes* in the *middle* and *bottom rows*.

regions (such as individual clock-hours) when compared with a global parameter.[18]

A consideration of how to interpret the longitudinal SNRs used in this study is also required to understand the implications of the findings. Note that the longitudinal SNR is a normalized measure of rate of change (y^{-1}). That is, it is an age-corrected rate of RNFL thickness change per year divided by the standard deviation of test-retest differences. As such, this measure should not be used to interpret whether an individual eye has progressed or not (as conventional SNRs or *z*-scores would typically be used), but simply as a normalized measure to compare the performance of the different methods for detecting change relative to variability. However, when comparing different methods, this continuous measure can be used in a population-based analysis to provide substantially greater statistical power as compared with an individual-based, dichotomized outcome measure of progression status.[19] This is particularly advantageous given that a majority of glaucoma eyes under routine clinical care progress slowly,[20] and the true potential value of a new method may be obscured with individual-based analyses, which require large patient cohorts evaluated over a long follow-up duration to be sufficiently powered. Nonetheless, the implication of such an analysis is that the interpretations of our findings are only population-based (although powerful for proof-in-principle), and thus require future investigations at the individual level.

Recognizing how to interpret the longitudinal SNRs and its analyses, this study showed in a substantially larger cohort than our previous studies[7,8] that a manual ROI approach indeed allows progressive cpRNFL thickness changes to be better captured than a global metric. Even though this was a similar trend when using the automatic ROI method, this did not reach statistical significance in this study. The difference in this finding from our previous studies[7,8] is most likely attributed to the fact that measurement variability and age-related changes were carefully accounted for in this study and/or differences in the populations studied. For example, only

eyes with disc hemorrhages were included in our first study.[7]

Nonetheless, the detection of disease progression was superior through the manual identification of ROIs. This is likely due in part to the fact that not all regions of glaucomatous damage can be sufficiently captured or identified using the automatic ROI approach, as shown in examples in Figure 5. This is most likely attributed to normal interindividual variations in both the cpRNFL thickness profile and its overall thickness.[21–23] For instance, a localized cpRNFL defect would be more likely to fall below the 1% lower normative limits in an eye where the overall prediseased cpRNFL thickness was lower than an eye where it was higher.

The superiority of the manual ROI approach highlights the potential for the improvement in the power to detect progressive cpRNFL thickness changes on OCT imaging through a careful qualitative (manual) evaluation of its results, in a similar manner to a careful examination of the optic nerve appearance on fundus biomicroscopy. This is contrasted with a reliance on summary measures or alerts of disease progression using current methods[4–6] that are agnostic to the nature and patterns of progressive glaucomatous damage. However, we note that this potential advantage is inferred from the findings at a population-based level, and future studies are required to better understand the implications of these advantages at an individual level. Nonetheless, the findings of this study also highlight a need for the improvement of automated methods. For instance, the automatic ROI approach in this study could be improved through reducing the interindividual variability of the cpRNFL thickness profile using anatomic features and biometric parameters,[23] which in turn can allow disease-related changes to be better distinguished from normal variations. Furthermore, the use of artificial intelligence (e.g., deep learning methods) in the evaluation of the OCT scan information could also contribute to this task, as we have recently shown for the detection of glaucomatous damage.[24]

A limitation of this study is that only two visits were included when evaluating disease progression, although increasing the number of visits would simply improve the precision of the change estimates without affecting the conclusions of this study. Another possible limitation is the use of within-session estimates of measurement variability instead of short-term between-visit estimates, although this would also not be expected to affect the conclusions from this study because the variability estimates for each method, which acted as the common denominator for the longitudinal SNRs, were obtained from the same eyes. This study also used age-related change estimates obtained from a different OCT device than the one used in the longitudinal and variability groups, although the protocol and scanning procedure was practically identical and the only important difference being the scanning speeds of the two devices. This is unlikely to have a significant impact on the estimates of age-related change of the RNFL thickness, and also the conclusions of this study because the age-related change estimates for each method evaluated in this study was also obtained from the same eyes. It is also possible that the generalizability of the manual ROI approach is limited by the experience of the examiner performing the grading. However, this study was intended as a proof-in-principle of an approach, which would require a validation of its generalizability of benchmarked examiners if applied more widely. Finally, this study simply revealed that a manual ROI approach allowed cpRNFL thickness changes to be better detected relative to measurement variability and normal age-related changes. However, it remains to be determined whether the changes detected with this approach also better predicts other clinical measures of progression, such as an expert masked assessment of optic disc stereophotographs or visual field progression, and future studies are required to examine this.

In conclusion, this study showed that the manual ROI approach—one that makes use of a prior knowledge of the nature of glaucomatous damage during the qualitative evaluation—was superior at detecting progressive cpRNFL thinning when compared with the conventional global measure and an automatic ROI approach. The findings of the present study underscore the potential advantages of making full use of the information available on OCT imaging in the challenging task of detecting progressive glaucomatous damage, in agreement with our previous observations that a qualitative evaluation is superior to summary metrics when detecting early glaucomatous damage.[9]

Acknowledgments

Supported by a National Institutes of Health Grant R01-EY-02115 (DCH), Lary Stromfeld Research Fund of NYEEI (RR), and a National Health

and Medical Research Council Early Career Fellowship #1104985 (ZW).

Disclosure: **Z. Wu**, None; **A. Thenappan**, None; **D.S.D. Weng**, None; **R. Ritch**, None; **D.C. Hood**, Topcon, Inc (F, C), Heidelberg Engineering (F)

References

1. Ramulu P. Glaucoma and disability: which tasks are affected, and at what stage of disease? *Curr Opin Ophthalmol*. 2009;20:92.
2. Medeiros FA. How should diagnostic tests be evaluated in glaucoma? *Br J Ophthalmol*. 2007;91: 273–274.
3. Medeiros FA, Zangwill LM, Bowd C, Sample PA, Weinreb RN. Use of progressive glaucomatous optic disk change as the reference standard for evaluation of diagnostic tests in glaucoma. *Am J Ophthalmol*. 2005;139:1010–1018.
4. Vianna JR, Chauhan BC. How to detect progression in glaucoma. *Prog Brain Res*. 2015;221: 135–158.
5. Yu M, Lin C, Weinreb RN, et al. Risk of visual field progression in glaucoma patients with progressive retinal nerve fiber layer thinning: a 5-year prospective study. *Ophthalmology*. 2016; 123:1201–1210.
6. Lin C, Mak H, Yu M, Leung CK-S. Trend-based progression analysis for examination of the topography of rates of retinal nerve fiber layer thinning in glaucoma. *JAMA Ophthalmol*. 2017; 135:189–195.
7. Hood DC, Xin D, Wang D, et al. A region-of-interest approach for detecting progression of glaucomatous damage with optical coherence tomography. *JAMA Ophthalmol*. 2015:1–7.
8. Thenappan A, De Moraes CG, Wang DL, et al. Optical coherence tomography and glaucoma progression: a comparison of a region of interest approach to average retinal nerve fiber layer thickness. *J Glaucoma* 2017;26:437–477.
9. Hood DC. Improving our understanding, and detection, of glaucomatous damage: an approach based upon optical coherence tomography (OCT). *Prog Retin Eye Res*. 2017;57:46–75.
10. Leung CK-S, Ye C, Weinreb RN, et al. Impact of age-related change of retinal nerve fiber layer and macular thicknesses on evaluation of glaucoma progression. *Ophthalmology*. 2013;120:2485–2492.
11. Vianna JR, Danthurebandara VM, Sharpe GP, et al. Importance of normal aging in estimating the rate of glaucomatous neuroretinal rim and retinal nerve fiber layer loss. *Ophthalmology*. 2015;122: 2392–2398.
12. Wu Z, Saunders LJ, Zangwill LM, et al. Impact of normal aging and progression definitions on the specificity of detecting retinal nerve fiber layer thinning. *Am J Ophthalmol*. 2017;181:106–113.
13. Leung CK-S, Cheung CY-l, Weinreb RN, et al. Retinal nerve fiber layer imaging with spectral-domain optical coherence tomography: a variability and diagnostic performance study. *Ophthalmology*. 2009;116:1257–1263. e2.
14. Garas A, Vargha P, Holló G. Reproducibility of retinal nerve fiber layer and macular thickness measurement with the RTVue-100 optical coherence tomograph. *Ophthalmology*. 2010;117:738–746.
15. Mwanza J-C, Chang RT, Budenz DL, et al. Reproducibility of peripapillary retinal nerve fiber layer thickness and optic nerve head parameters measured with cirrus HD-OCT in glaucomatous eyes. *Invest Ophthalmol Vis Sci*. 2010;51:5724–5730.
16. Hood DC, Fortune B, Mavrommatis MA, et al. Details of glaucomatous damage are better seen on oct en face images than on oct retinal nerve fiber layer thickness maps. *Invest Ophthalmol Vis Sci*. 2015;56:6208–6216.
17. Gardiner SK, Fortune B, Demirel S. Signal-to-noise ratios for structural and functional tests in glaucoma. *Trans Vis Sci Tech*. 2013;2(6):3.
18. Chauhan BC, Danthurebandara VM, Sharpe GP, et al. Bruch's membrane opening minimum rim width and retinal nerve fiber layer thickness in a normal white population: a multicenter study. *Ophthalmology*. 2015;122:1786–1794.
19. Royston P, Altman DG, Sauerbrei W. Dichotomizing continuous predictors in multiple regression: a bad idea. *Stat Med*. 2006;25:127–141.
20. Chauhan BC, Malik R, Shuba LM, et al. Rates of glaucomatous visual field change in a large clinical population. *Invest Ophthalmol Vis Sci*. 2014;55:4135–4143.
21. Hood DC, Kardon RH. A framework for comparing structural and functional measures of glaucomatous damage. *Prog Retin Eye Res*. 2007;26:688–710.
22. Denniss J, Turpin A, McKendrick AM. Visual contrast detection cannot be predicted from surrogate measures of retinal ganglion cell number and sampling density in healthy young adults. *Invest Ophthalmol Vis Sci*. 2014;55:7804–7813.

23. Pereira I, Resch H, Schwarzhans F, et al. Multivariate model of the intersubject variability of the retinal nerve fiber layer thickness in healthy subjects. *Invest Ophthalmol Vis Sci*. 2015;56:5290–5298.

24. Muhammad H, Fuchs TJ, De Cuir N, et al. Hybrid deep learning and a single wide-field oct scan accurately classifies glaucoma suspects. *J Glaucoma*. 2017;26:1086–1094.